Three different types of physical gels originate from a common triblock copolymer precursor: The case of an ionomer gel

ARTICLE · FEBRUARY 2013

DOI: 10.1039/C2PY21024J

4 AUTHORS, INCLUDING:

Zacharoula Iatridi
University of Patras
21 PUBLICATIONS **184** CITATIONS
SEE PROFILE

Constantinos Tsitsilianis
University of Patras
129 PUBLICATIONS **2,558** CITATIONS
SEE PROFILE

Polymer Chemistry

RSC Publishing

PAPER

Three different types of physical gels originate from a common triblock copolymer precursor: the case of an ionomer gel

Cite this: *Polym. Chem.*, 2013, **4**, 2097

Nikoletta Stavrouli,[ab] Zacharoula Iatridi,[a] Thierry Aubry[c] and Constantinos Tsitsilianis*[ab]

Received 23rd November 2012
Accepted 29th December 2012

DOI: 10.1039/c2py21024j

www.rsc.org/polymers

We report the self-assembly of a triblock ionomer consisting of a long poly(2-vinyl pyridine) end-capped by fully neutralized poly(acrylic acid) (PANa-*b*-P2VP-*b*-PANa) in methanol which is a selective solvent of P2VP. This polymer arises from a P*t*BA-*b*-P2VP-*b*-P*t*BA triblock precursor by acid hydrolysis and subsequent neutralization by MeONa. The PANa-*b*-P2VP-*b*-PANa self-assembles through dipole interactions forming flower-like micelles, comprising a great number of ion pairs and P2VP looping chains. As the concentration increased, loop to bridge transitions led to the formation of a transient network. The so-formed physical gel exhibited a percolation concentration at 1.6 wt% and relaxation times of the order of several hundreds of seconds. The present work shows that all the types of ionogenic physical gels, *i.e.* polyelectrolyte, polyampholyte, ionomer, can be afforded from a common triblock copolymer precursor. The resulting physical gels arise from different types of interactions, *i.e.* hydrophobic, electrostatic, dipoles, which determine the structural features of the formed transient network and in turn its rheological properties.

1 Introduction

Macromolecules bearing attractive groups that can develop physical bonds through intermolecular association belong to a broad class of polymeric species named "associative" polymers (APs). The consequence of self-organization of these polymers when dissolved in a selective solvent is the creation of temporary networks which impart specific rheological properties attracting considerable interest in numerous applications in the fields of cosmetics, pharmaceutics, coatings, *etc.*[1–5] APs include an important class of macromolecules, namely charged polymers, which can be distinguished into three subclasses: polyelectrolytes,[5–21] polyampholytes[22–26] and ionomers.[27–37]

As far as ionomers are concerned, their structure and rheological properties in media of low dielectric constant have been the object of several studies mainly because of their potential interest as rheology modifiers (viscosity enhancers as well as shear-thickening and shear-thinning agents) in low polarity solvents.[31–37] These linear and non-linear rheological properties are due to the formation of a reversible network above a certain polymer concentration, where polar associations act as temporary junctions. More precisely, these associations are organized in microdomains, the so-called multiplets, through polar interactions mediated by ion pairs composed of non-dissociated counterions bound to ions of the polymer chains.[38,39]

Particular attention has been paid to block ionomer association[40] which leads to micelles with much higher stability than that of micelles formed by nonionic copolymers, due to the strong dipole interactions.[41] Eisenberg *et al.* have extensively studied the self-assembly behaviour of diblock ionomers, *i.e.* copolymers constituted of a nonionic block (polystyrene) and a shorter ionic block, *e.g.* neutralized poly(acrylic acid) (PAA)[42] or poly(methacrylic acid) (PMAA)[43] or quaternized P4VP.[44] When dissolved in an organic solvent of low polarity, these ionomers form very stable reverse micelles with an ionic core surrounded by a nonionic corona. The structure of the micelles was shown to be affected by the neutralization degree, the block copolymer composition, the nature of the solvent and the metal ion as well as the preparation method.

BAB triblock copolymers, with B ionomer blocks, form physical gels in which again the structure and the rheological properties depend on the preparation method, the nature of the solvent and the ionization degree.[45–48] The self-assembly of a partially sulfonated polystyrene-*b*-poly(ethylene-*co*-butyrene)-*b*-polystyrene (SEBS) triblock ionomer was studied by Weiss *et al.*[49] who have shown that the ionomer chains could organize into various structures like deformed spheres, cylinders or lamellae, which were affected by the sample preparation

[a]*Department of Chemical Engineering, University of Patras, 26504, Patras, Greece. E-mail: ct@chemeng.upatras.gr*

[b]*Institute of Chemical Engineering Sciences, ICE/HT-FORTH, P.O. Box 1414, 26504 Patras, Greece*

[c]*Equipe Rhéologie, LIMATB, U.F.R. Sciences et Techniques, Université de Bretagne Occidentale, 6 avenue Victor Le Gorgeu, CS 93837 29238 Brest Cedex 3, France*

method, degree of ionization or type of cations used. Another sulfonated SEBS triblock ionomer was studied in THF by Wu *et al.*[50] using light scattering experiments. The results showed that the dissolution process of the three-dimensional network formed through the linking by ion-pair multiplets of sulfonated SEBS chains depended on the strength of the linkage.

The association mechanism of end-functionalized halatotelechelic ionomers in apolar solvents towards a transient network was also studied previously. Above the critical aggregation concentration (CAC) the ionic groups interacted, forming multiplets. The formed micelles adopted a flower-like assembly comprising four macromolecules. As the concentration increased, the number of flower-like micelles increased and above a certain micelle concentration, further association *via* bridging into larger aggregates was observed leading to a transient network at even higher ionomer concentration.[37]

In this paper we will show for the first time that it is possible to come up with the three types of ionic associative triblock copolymers (polyelectrolyte, polyampholyte and ionomer) from the same common copolymer precursor. The poly(*tert*-butyl acrylate)-*b*-poly(2-vinyl pyridine)-*b*-poly(*tert*-butyl acrylate) triblock copolymer constitutes the first paradigm of such multifunctional triblock copolymers. Scheme 1 demonstrates the three pathways that lead to different transient networks resulting from self-organization of the easily modified triblock precursor. In the first pathway, P*t*BA-*b*-P2VP-*b*-P*t*BA dissolved in acidic water behaves as a telechelic polyelectrolyte since the P2VP central block is ionized by protonation of the pyridine groups. A network is formed through hydrophobic interactions of the P*t*BA end-blocks.[25] In the second pathway, the P*t*BA end blocks are hydrolyzed yielding a double hydrophilic block polyampholyte (PAA-*b*-P2VP-*b*-PAA).[22,23] This polymer can form a network by electrostatic attractive interactions of oppositely charged moieties of PAA and protonated P2VP blocks in a pH window around pH 3.5. This pH window can be broadened by P2VP quaternization. Finally in the third pathway, the neutralized form of the hydrolyzed polymer, *i.e.* PANa-*b*-P2VP-*b*-PANa, behaves as an associative triblock ionomer in organic solvents *e.g.* methanol (MeOH), forming a transient network through dipole interactions of the ion pairs of the PANa end-blocks. The first two cases have been reported previously while the ionomer case is the subject of the present work.

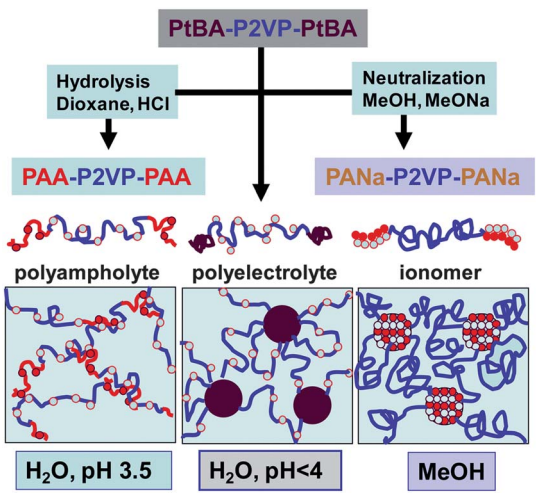

Scheme 1 Schematic representation of three pathways leading to different three-dimensional nanostructures originating from the same triblock copolymer precursor. From left to right: polyampholyte gel through electrostatic interactions, polyelectrolyte gel through hydrophobic interactions and ionomer gel through dipole interactions. The closed and open red circles denote negative and positive ions, respectively.

2 Experimental part

Synthesis

The P*t*BA-*b*-P2VP-*b*-P*t*BA triblock copolymer was synthesized by "living" anionic polymerization, using sodium tetraphenyl diisobutane as a bifunctional organometallic initiator, so as to achieve symmetrical chain growth at both active ends. The reaction was carried out in THF solution, under an argon atmosphere at −78 °C and −65 °C, during the addition/reaction of 2-vinyl pyridine and *tert*-butyl acrylate, respectively. Experimental details of the synthetic procedure have been reported elsewhere.[22]

The postpolymerization reaction of acid catalyzed hydrolysis of the P*t*BA to PAA blocks was carried out in 1,4-dioxane with 10-fold excess of fuming hydrochloric acid 37% (wt/wt), at 80 °C for 24 hours. The molecular characteristics of the copolymer under investigation are summarized in Table 1.

Size Exclusion Chromatography (SEC)

Size exclusion chromatography was performed, using PL gel columns of different pore size and an RI-detector, in order to determine the molecular weight distribution of the precursor P2VP and the P*t*BA-*b*-P2VP-*b*-P*t*BA triblock copolymer. The mobile phase was 1% triethylamine solution in tetrahydrofuran and flow rate 0.5 ml min^{-1}.

Nuclear Magnetic Resonance (NMR)

^{1}H-NMR spectra were measured on a Bruker AC-400 spectrometer using $CDCl_3$ and a d_6-methanol–$CDCl_3$ mixture, as deuterized solvents for precursor (P*t*BA-*b*-P2VP-*b*-P*t*BA) and hydrolyzed copolymer (PAA-*b*-P2VP-*b*-PAA), respectively. NMR measurements were used in order to determine the percentage of the different species that constitute the copolymer, as well as the degree of hydrolysis of the final product and the exact molecular weight of both samples.

Static Light Scattering (SLS)

The molecular weight of the P2VP central block was determined by SLS measurements using a thermally regulated (±0.1 °C) spectro-goniometer, Model BI-200SM (Brookhaven), equipped with a He–Ne laser (632.8 nm).

Dynamic Light Scattering (DLS)

Autocorrelation functions were measured with a Brookhaven BI-9000AT/Turbocorr digital correlator from a light source of a He–Ne laser (632.8 nm). CONTIN analysis was performed through

Table 1 Molecular characteristics of PAA-*b*-P2VP-*b*-PAA

Polymer	M_w[a]	M_w/M_n[b]	P2VP[c] (wt%)	P2VP DP_w[d]	P*t*BA/PAA (wt%)	P*t*BA/PAA DP_w[d]
P2VP	147 000	1.29				
(P*t*BA-*b*-P2VP-*b*-P*t*BA)	192 000	1.31	76.6	1397	23.4	175
(PAA-*b*-P2VP-*b*-PAA)	173 000		85	1397	1.1/13.9	12/163

[a] By SLS. [b] By SEC. [c] By H^1 NMR. [d] DP_w: degree of polymerization.

BI-DLSW software. The apparent hydrodynamic radius was determined *via* the Stokes–Einstein equation:

$$R_h = k_B T/6\pi\eta D_{app} \quad (1)$$

where D_{app} is the diffusion coefficient, k_B is the Boltzmann constant and η is the viscosity of the solvent at absolute temperature T.

Rheometry

The linear and non-linear rheological experiments were performed using three rotational rheometers:

- a stress controlled Rheometrics Scientific SR200 rheometer, equipped with either a cone and plate geometry (diameter 25 mm, cone angle 5.7°, truncation 56 μm) or a Couette geometry (gap 1.1 mm) for the less viscous solutions.

- a stress controlled GEMINI Bohlin rheometer with a cone and plate geometry (diameter 40 mm, cone angle 4°, truncation 150 μm) for the more viscous solutions.

- a strain controlled Rheometrics Scientific ARES rheometer, equipped with a parallel-plate geometry (diameter 20 mm, gap 2 mm), for the stress relaxation measurements.

Geometries with rough surface of roughness ~0.2 mm were used in order to avoid slip. A thin layer of low viscosity silicone oil was put on the air–sample interface in order to minimize water evaporation. After each sample loading, the normal force was monitored, and no measurement was carried out, before complete relaxation of the sample. All rheological tests were performed at 25 °C.

Sample preparation

The triblock copolymer was dissolved in MeOH at room temperature (20–25 °C). In the following, quantitative neutralization of PAA units was carried out by adding sodium methoxide (CH_3ONa) 0.5 M.

3 Results

The first part of the present work deals with the characterization of the self-assemblies originating from the expected association of the PANa-*b*-P2VP-*b*-PANa triblock ionomer in dilute MeOH solutions (sol state), as MeOH is a good solvent for the central P2VP block and non-solvent for the outer ionic PANa blocks. The second part focuses on the rheological properties of the more concentrated solutions where a gel state appeared.

3.1 Self-organization in the sol state

The time relaxation distributions at 90° for eight different polymer concentrations, obtained by CONTIN analysis of autocorrelation functions, are presented in Fig. 1. At low concentrations (*i.e.* at $C = 0.01$ wt%), a rather broad unimodal distribution of relaxation times was observed. As the polymer concentration increased, a second peak corresponding to higher relaxation times appeared which was shifted to longer times with concentration.

In order to elucidate the origin of these two relaxation modes, the 1 wt% solution was studied at different scattering wave vectors, $\boldsymbol{q}$. The autocorrelation functions along with the distribution of relaxation times at various angles are presented in Fig. 2. As can be seen, the fast and the slow relaxation modes exhibit angular dependence.

In Fig. 3, the relaxation rates, $\Gamma = 1/\tau$, for both relaxation modes were plotted as a function of $\boldsymbol{q}^2$. In both cases, the relaxation process follows a diffusive character, as Γ is $\boldsymbol{q}^2$ dependent at low $\boldsymbol{q}$. Thus, the two peaks correspond to two populations of different size particles. From the slope at low $\boldsymbol{q}$ values, the translational diffusion coefficients D_0 of the particles were calculated, *i.e.* 2.21×10^{-11} m^2 s^{-1} and 4.96×10^{-13} m^2 s^{-1} for the first (Fig. 3a) and the second (Fig. 3b) population, respectively.

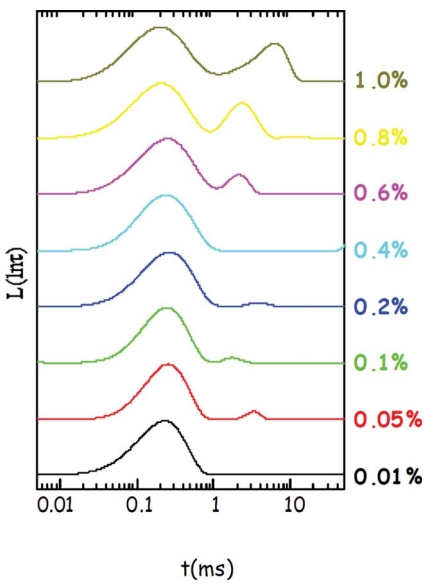

Fig. 1 Relaxation time distributions, $L(\ln \tau)$, for different concentrations of the PANa-*b*-P2VP-*b*-PANa triblock copolymer in MeOH from an angle of 90° and at room temperature.

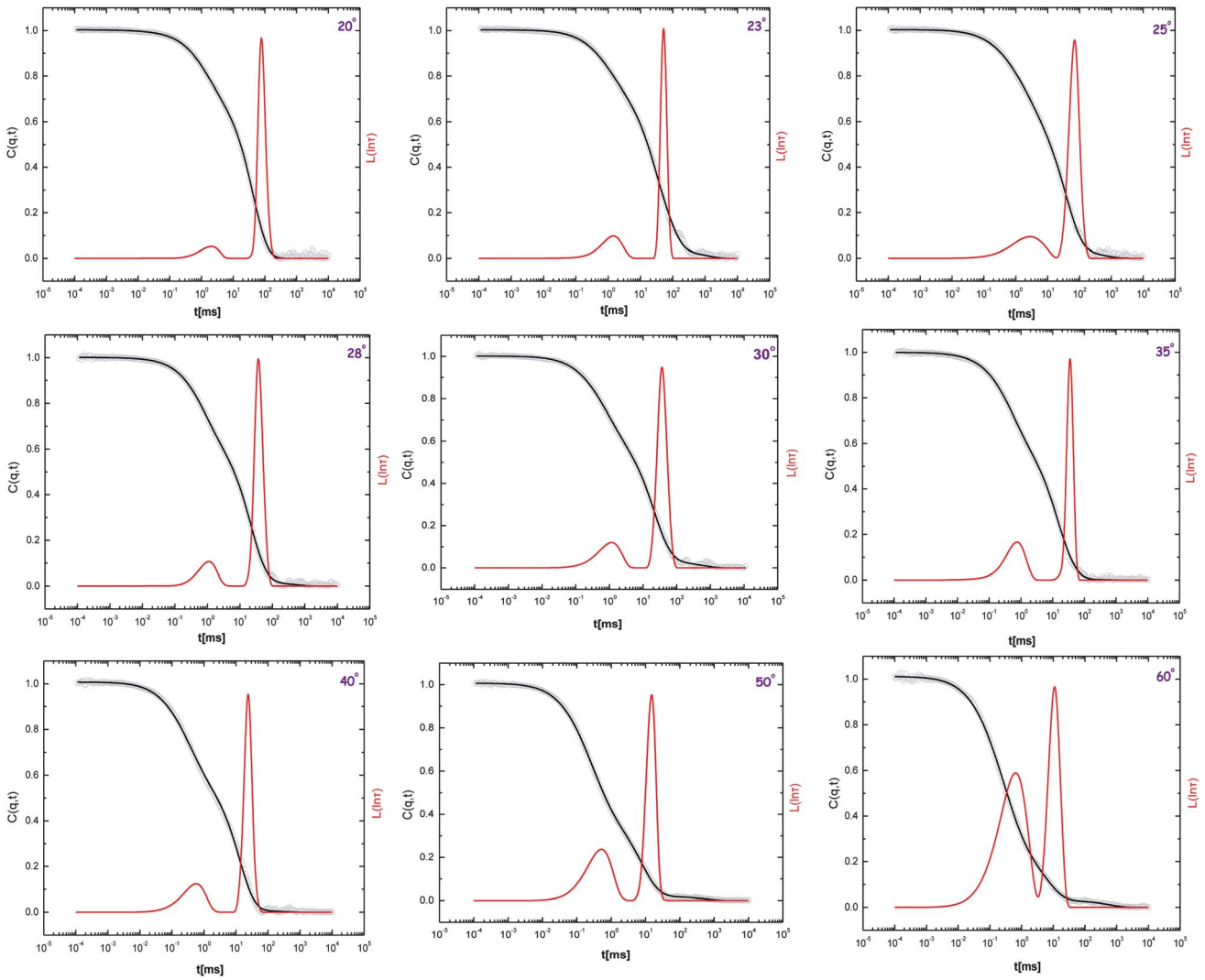

Fig. 2 Autocorrelation functions $C(\boldsymbol{q},t)$ and relaxation time distributions $L(\ln \tau)$ from different angle measurements of a 1.0 wt% solution of the PANa-*b*-P2VP-*b*-PANa ionomer in MeOH.

Correspondingly, the hydrodynamic radius R_h was calculated to be 9.7 nm and 430 nm, using the Stokes–Einstein equation (eqn (1)). Provided that block ionomers exhibit extremely low cmcs,[51] these results should be attributed to the existence of low size flower-like micelles and of large size clusters of bridged micelles respectively, as dictated by the triblock topology of the involved polymer. The clusters seem to grow with concentration as shown in Fig. 1, which eventually leads to an infinite cluster (network) as will be shown by rheological measurements. The observed supramolecular structures arise from the self-organization of the ionomer triblock copolymer through intermolecular association of the PANa end-blocks, driven by dipole interactions.

3.2 Rheological properties of the gel state

3.2.1 Steady shear. The flow curves of PANa-*b*-P2VP-*b*-PANa in MeOH solutions over a concentration range from 0.8 wt% up to 3.2 wt% have been plotted in Fig. 4. The results show that the solutions behave as Newtonian fluids for polymer concentrations below 1.6 wt%. Above 1.6 wt%, there is a very drastic enhancement of the zero-shear Newtonian viscosity and the appearance of a very marked shear-thinning behaviour at moderate shear stresses, which looks like a near discontinuity in the viscosity *versus* shear stress curve. Such features are quite common in the flow curve of associative polymeric systems and are classically attributed to the formation of a three-dimensional transient network, above a critical concentration. The dramatic shear-thinning behaviour at some moderate shear stress has been attributed to a catastrophic break up of the network.[52] For systems exhibiting very long relaxation times, which look like frozen systems on experimental time scales, the network eventually breaks up into a suspension of densely packed swollen microgels.[19,53]

In the case of the PANa-*b*-P2VP-*b*-PANa–MeOH system studied in this work, the steady-shear behaviour plotted in Fig. 4 can be attributed to the association of (flower-like) micelles into larger aggregates upon increasing polymer concentration. This

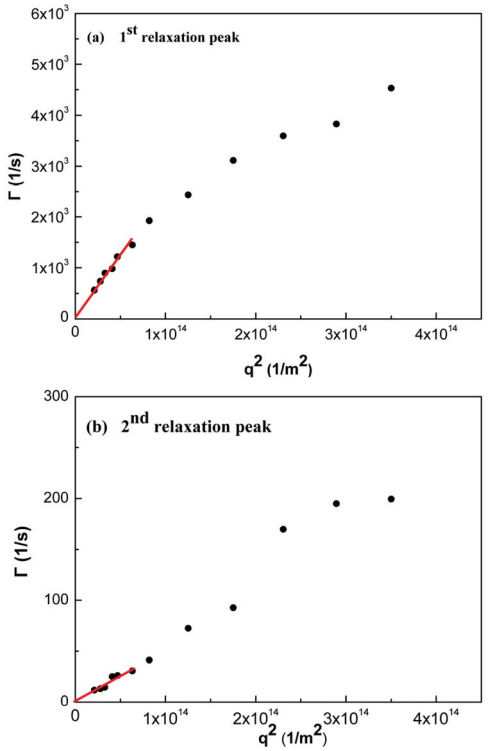

Fig. 3 q^2 dependence of relaxation rate, Γ, for the fast (a) and slow (b) relaxation peaks of a 1.0 wt% PANa-*b*-P2VP-*b*-PANa solution in MeOH. The lines are fits of the linear dependence in the low q limit.

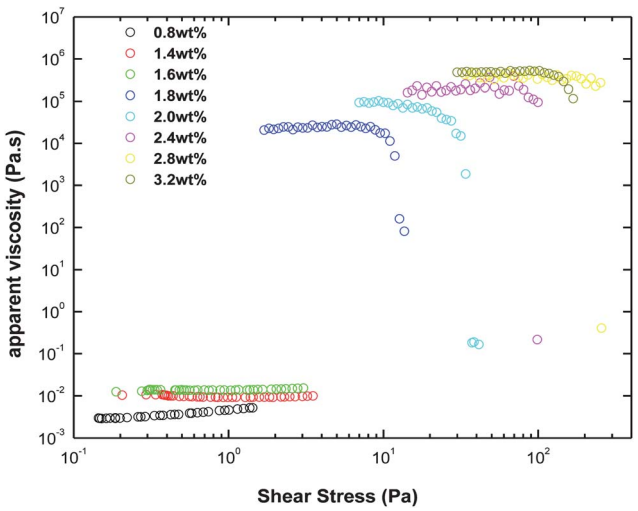

Fig. 4 Apparent viscosity as a function of shear stress for PANa-*b*-P2VP-*b*-PANa solutions in MeOH at various concentrations.

process leads *in fine*, above 1.6 wt%, to the formation of a space filling infinite aggregate composed of a 3D transient network whose junctions are formed by multiplets involving a great number of dipoles.

The assumption of the formation of a 3D physical network at high concentrations is confirmed in the inset of Fig. 5, which illustrates the typical solid-like (gel-like) behaviour observed for

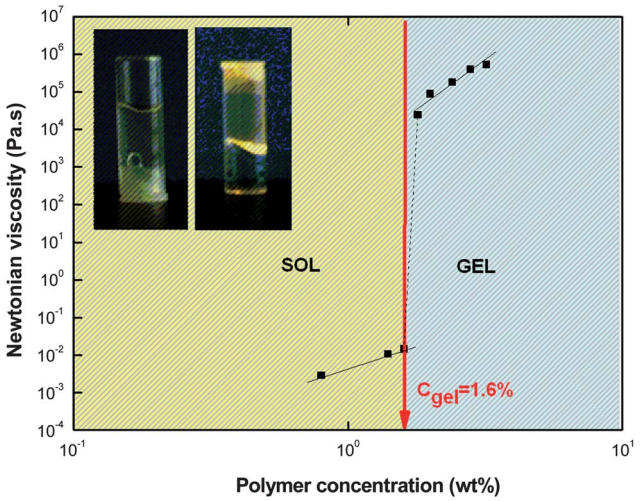

Fig. 5 Zero-shear Newtonian viscosity as a function of polymer concentration for PANa-*b*-P2VP-*b*-PANa in MeOH. Inset: illustration of a free standing gel after the inversion of the tube of a 2 wt% polymer concentration.

any PANa-*b*-P2VP-*b*-PANa–MeOH solution at polymer concentrations above 1.6 wt%. However, we would like to point out that the existence of a large, but quite easily measurable, zero-shear Newtonian viscosity for all gel-like systems studied in this work, shows that these systems are not kinetically frozen on the experimental time scales investigated in this work.

The zero-shear Newtonian viscosity as a function of polymer concentration is shown in Fig. 5. The results clearly confirm the existence of two concentration regimes separated by a concentration threshold $C_{gel} = 1.6$ wt%, which can be identified with gelation concentration. It should be noticed that the viscosity of the system increases quite steeply, more than five orders of magnitude in a narrow polymer concentration range, defining a concentration induced sol–gel transition. This behavior is not so frequent in associative polymer solutions.

3.2.2 Oscillatory shear. Fig. 6 shows the storage and loss moduli of PANa-*b*-P2VP-*b*-PANa in MeOH as a function of strain at 0.5 Hz and at a polymer concentration above C_{gel}. The extent of the linear viscoelastic regime is about 50%; this rather large value of critical strain could be ascribed to the stretchability of the flexible P2VP central blocks in MeOH. Moreover a strain hardening effect can be seen as G' increases with strain prior to its sharp decrease. This effect could be attributed to chain stretching upon applying high deformation.[36,54]

The frequency dependence of viscoelastic moduli G' and G'' is plotted in Fig. 7 for a 2.4 wt% PANa-*b*-P2VP-*b*-PANa gel in methanol. It is representative of the frequency sweep viscoelastic results obtained from all ionomer gels studied in this work. Fig. 7 shows that the storage modulus G' and the loss modulus G'' are nearly constant over at least two frequency decades (from 10^{-2} to 1 Hz), with $G' \gg G''$, underlying the solid-like (gel-like) behaviour at polymer concentrations above C_{gel}.

It is worth noticing that such a rheological behaviour defers remarkably from that of telechelic ionomers (with only one ion pair at both chain ends) in nonpolar solvents which behaves as

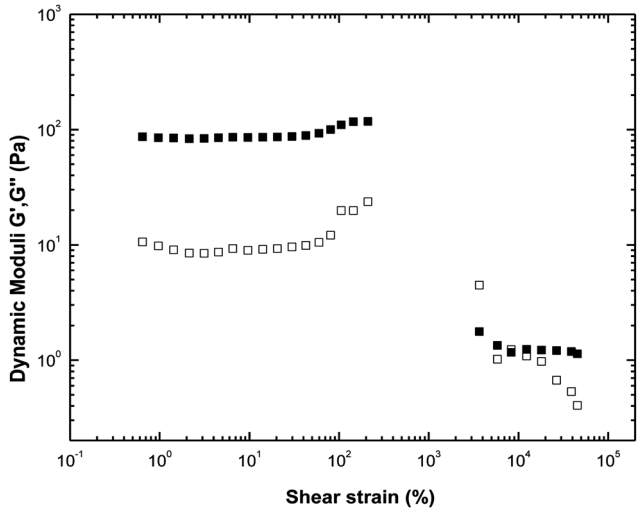

Fig. 6 Dynamic moduli G' and G'' as a function of strain for 2.4 wt% PANa-*b*-P2VP-*b*-PANa in MeOH.

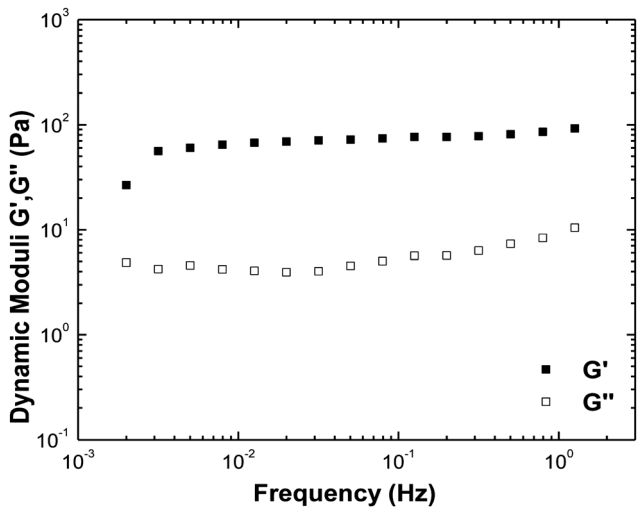

Fig. 7 Dynamic moduli G' and G'' as a function of frequency in the linear viscoelastic regime, for a 2.4 wt% PANa-*b*-P2VP-*b*-PANa gel in MeOH.

a liquid at low frequencies ($G'' > G'$) and as a gel at higher frequencies.[37] However, the linear viscoelastic behaviour on long time scales, characterized by a significant tendency for G' increase with frequency at the lowest frequencies investigated in this work (Fig. 7), suggests that the system behaves as a viscoelastic fluid and eventually flows on a long time scale ($\sim 10^3$ s). The viscoelastic behaviour observed for triblock ionomer gels could be attributed to the large number of dipoles involved in the multiplets, leading to a large exchange time of end-blocks between the multiplets, and therefore to viscoelastic fluid like behaviour on long time scales and solid like behaviour on short or moderate time scales.

The plateau viscoelastic moduli *versus* polymer concentration are plotted in Fig. 8, for PANa-*b*-P2VP-*b*-PANa in MeOH gels. Fig. 8 shows that the concentration dependence of the plateau storage modulus $G_0^{'}$ and the plateau loss modulus $G_0^{''}$

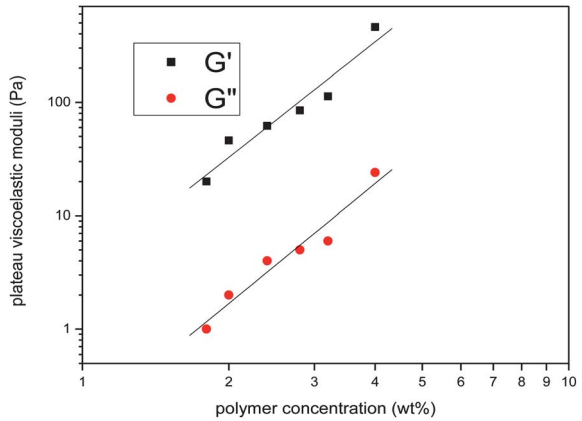

Fig. 8 Plateau storage and loss moduli G'_0 and G''_0 as a function of polymer concentration above the gelation concentration. Solid lines correspond to linear fit of the data.

can be described rather satisfactorily by the same power law function:

$$G_0^{'},\ G_0^{''} \sim c^{3.3} \tag{2}$$

Regarding the viscous dissipative properties of PANa-*b*-P2VP-*b*-PANa ionomer gels, eqn (2) also means that $G_0^{''}/G_0^{'}$ is independent of the polymer concentration: $G_0^{''}/G_0^{'} \sim 5\%$.

Using the Green–Tobolsky model, the fraction f of elastically effective chains in the physically cross-linked network can be inferred from the value of the plateau storage modulus:[55]

$$f = G_0/Nk_BT \tag{3}$$

where N is the number density of polymer chains at a given polymer concentration, k_B is the Boltzmann constant and T the absolute temperature.

At a concentration of 1.8 wt%, that is just above the gelation threshold, it can be deduced (eqn (3)) that only ~8% polymer chains are elastically active in the network, which means that only a few polymer chains are needed to form a percolation network of bridged flower-like micelles. However, at a concentration of 4 wt%, the fraction of elastically active chains is about 10 times higher, *i.e.* ~80%, which indicates that increasing the polymer concentration promotes numerous conversions from loops to bridges, in qualitative agreement with the rather high exponent in eqn (2).

3.2.3 Stress relaxation. In order to evaluate the relaxation time of the system, a stress relaxation experiment was performed for a 4 wt% ionomer gel. In Fig. 9, the stress relaxation modulus is plotted as a function of time. The data have been fitted by a stretched exponential function (eqn (4)).

$$G(t) = G_0 \exp -(t/\tau)^{\alpha} \tag{4}$$

The best fit was obtained with the following parameters: the instantaneous elastic modulus $G_0 = 560$ Pa, the exponent $\alpha = 0.17$ and the characteristic relaxation time $\tau = 620$ s.

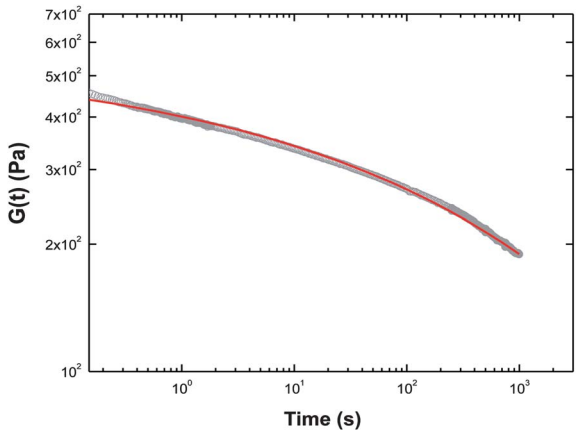

Fig. 9 Stress relaxation of a 4 wt% PANa-*b*-P2VP-*b*-PANa solution in MeOH at a strain of 10%. The best fit (in red) corresponds to a stretched exponential function.

The existence of a long characteristic relaxation time, which can be related to the exchange time of end-blocks between the multiplets, confirms the results deduced from the oscillatory measurements which highlighted the prominent role played by the strong dipole interactions resulted from the presence of a great number of ion pairs within multiplets (network junctions). However as already pointed out, the existence of a large but experimentally accessible governing relaxation time means that the dynamic exchange of end-blocks between multiplets takes place in the system within the time scale of rheometrical experiments. Besides, the low value of the stretched exponent α means that the distribution of relaxation times is broad, suggesting some variability in the multiplet structures likely due to size polydispersity of the end-blocks.

4 Discussion

After demonstrating the rheological properties of the ionomer gel, we attempt a comparison of the three gel systems originating from the same triblock precursor *i.e.* polyelectrolyte (elec.) gel, polyampholyte (amph.) gel and ionomer (ion.) gel. As we have shown in Scheme 1, the three associative triblock copolymers form structured fluids, when dissolved in appropriate solvents that do not flow above a certain polymer concentration. The polymeric structures responsible for the gel formation arise from different types of interactions *e.g.* hydrophobic, electrostatic, and dipole interactions, for polyelectrolyte, polyampholyte and ionomer gels respectively, which lead to different rheological properties.

The percolation concentration (denoted as C_{gel}) of the three polymeric systems follows the order: $C_{gel}^{elec.} < C_{gel}^{amph.} < C_{gel}^{ion.}$. Indeed, from the concentration dependence of the viscosity of the polyampholyte system (results not shown) it appears that the gelation concentration of the ionomer in MeOH is about 4 times higher than that of the polyampholyte, which in turn is higher than that of the polyelectrolyte in water (pH 3.7) as shown previously.[25] The number of polymeric chains needed to fill up the space depends on the effective length (conformation) of the solvophilic central block (P2VP) and the size of the physical crosslinking domains (aggregation number of multiplets). It seems that for the polymer system with the highest C_{gel}, the size of the multiplets in the gel phase should be the largest as expected from the high number of dipoles of the PANa end-blocks, which has also been observed in other systems (*e.g.* PS-PANa–DMF).[43]

The features of the three polymer gels also appear to be quite different. First of all, the strain dependence of G' and G'' reveals a very narrow linear viscoelastic regime for the polyelectrolyte gel. Indeed, the critical γ_c above which the system flows is of the order of 1%, meaning that this gel is "fragile", although the physical crosslinks are "frozen" as the P*t*BA chain ends are long and highly hydrophobic. On the other hand, the polyampholyte and ionomer gels exhibit γ_c at about 50%. Moreover, strain hardening effects were observed, which are more pronounced for the polyampholyte system. The latter could be attributed to the double solvophilic nature of PAA and P2VP segments allowing the existence of dangling ends which can be mechanically forced to contribute to the network, increasing therefore the elastic modulus. The "fragility" of the polyelectrolyte network was thought to arise from the stretched conformation of the elastic chains.[25] In recent reports it was considered that in the case of hydrophobically end-capped polyelectrolytes with highly hydrophobic end-blocks (like the present triblock), the formed nanostructure might not be an infinite 3D network but rather a suspension of densely packed swollen finite clusters (microgels), due to extremely slow dynamics of the hydrophobic end-blocks.[17,19,53] On the other hand, the ionomer gel exhibits relaxation times of the order of hundreds of seconds, suggesting that this system is more dynamic even if it looks "frozen" on lower time scales. Similar behavior in terms of relaxation times was observed for the polyampholyte system. Finally, the elastic modulus, well above the percolation threshold, exhibits the following order: $G_0^{elec.} > G_0^{ion.} > G_0^{amph.}$. In the case of polyelectrolyte gels, it has to be noticed that G_0 exceeds significantly the value of a fully elastic network derived from eqn (3).[8,9]

5 Conclusions

In this article we have studied the association behavior of a fully neutralized PAA-*b*-P2VP-*b*-PAA triblock copolymer in MeOH, which is a selective solvent for the central block. The triblock ionomer self-assembles through dipole interactions of the ion pairs of the PANa end-blocks, forming flower-like micelles that further associate through bridging into clusters, leading eventually to a three dimensional transient network at elevated concentrations.

The rheological investigation of the so-formed ionomer gel was accomplished by a steady state and oscillatory shear as well as stress relaxation measurements. Above a percolation threshold, $C_{gel} = 1.6$ wt%, the viscosity was dramatically increased by more than five orders of magnitude, revealing the formation of a 3D transient network constituting physical

crosslinks involving a great number of dipoles bridged by P2VP solvophilic elastic chains. The ionomer network was characterized by a broad distribution of relaxation times with a mean value of the order of several hundreds of seconds, which classifies this system at the limit between dynamic and frozen physical gels.

The present work is the third part of a trilogy, showing that all the types of ionogenic physical gels, *i.e.* polyelectrolyte, polyampholyte, ionomer, can be afforded from a common triblock copolymer through an easy modification of the end-blocks. The resulting physical gels arise from different types of interactions, *i.e.* hydrophobic, electrostatic, dipoles, which determine the structural features of the formed transient network affecting remarkably the rheological properties of the physical gel.

References

1 M. A. Winnik and A. Yekta, *Curr. Opin. Colloid Interface Sci.*, 1997, **2**, 424.
2 M. Rubinstein and A. V. Dobrynin, *Trends Polym. Sci.*, 1997, **5**, 181.
3 J. F. Berret, D. Calvet, A. Collet and M. Viguier, *Curr. Opin. Colloid Interface Sci.*, 2003, **8**, 296.
4 C. Tsitsilianis, *Soft Matter*, 2010, **6**, 2372.
5 C. Chassenieux, T. Nicolai and L. Benyahia, *Curr. Opin. Colloid Interface Sci.*, 2011, **16**, 18.
6 V. V. Vasilevskaya, I. I. Potemkin and A. R. Khokhlov, *Langmuir*, 1999, **15**, 7918.
7 C. Tsitsilianis, I. Iliopoulos and G. Ducouret, *Macromolecules*, 2000, **33**, 2936.
8 C. Tsitsilianis and I. Iliopoulos, *Macromolecules*, 2002, **35**, 3662.
9 I. Katsampas and C. Tsitsilianis, *Macromolecules*, 2005, **38**, 1307.
10 G. T. Gotzamanis, C. Tsitsilianis, S. C. Hadjiyannakou, C. S. Patrickios, R. Lupitskyy and S. Minko, *Macromolecules*, 2006, **39**, 678.
11 Y. D. Zaroslov, G. Fytas, M. Pitsikalis, N. Hadjichristidis, O. E. Philippova and A. R. Khokhlov, *Macromol. Chem. Phys.*, 2005, **206**, 173.
12 I. Katsampas, Y. Roiter, S. Minko and C. Tsitsilianis, *Macromol. Rapid Commun.*, 2005, **26**, 1371.
13 S. A. Angelopoulos and C. Tsitsilianis, *Macromol. Chem. Phys.*, 2006, **207**, 2188.
14 F. Bossard, T. Aubry, G. Gotzamanis and C. Tsitsilianis, *Soft Matter*, 2006, **2**, 510.
15 R. Zhang, T. Shi, L. An, Z. Sun and Z. Tong, *J. Phys. Chem. B*, 2010, **114**, 3449.
16 R. Zhang, T. Shi, H. Li and L. An, *J. Chem. Phys.*, 2011, **134**, 034903.
17 C. Tsitsilianis, T. Aubry, I. Iliopoulos and S. Norvez, *Macromolecules*, 2010, **43**, 7779.
18 S. Hietala, S. Strandman, P. Jarvi, M. Torkkeli, K. Jankova, S. Hvilsted and H. Tenhu, *Macromolecules*, 2009, **42**, 1726.
19 C. Charbonneau, C. Chassenieux, O. Colombani and T. Nicolai, *Macromolecules*, 2011, **44**, 4487.
20 O. Borisova, L. Billon, M. Zaremski, B. Grassl, Z. Bakaeva, A. Lapp, P. Stepanek and O. Borisov, *Soft Matter*, 2011, **7**, 10824.
21 C. Charbonneau, C. Chassenieux, O. Colombani and T. Nicolai, *Macromolecules*, 2012, **45**, 1025.
22 V. Sfika and C. Tsitsilianis, *Macromolecules*, 2003, **36**, 4983.
23 F. Bossard, V. Sfika and C. Tsitsilianis, *Macromolecules*, 2004, **37**, 3899.
24 F. Bossard, C. Tsitsilianis, S. N. Yannopoulos, G. Petekidis and V. Sfika, *Macromolecules*, 2005, **38**, 2883.
25 N. Stavrouli, T. Aubry and C. Tsitsilianis, *Polymer*, 2008, **49**, 1249.
26 Z. Iatridi, G. Mattheolabakis, K. Avgoustakis and C. Tsitsilianis, *Soft Matter*, 2011, **7**, 11160.
27 S. Bhargava and S. L. Cooper, *Macromolecules*, 1998, **31**, 508.
28 C. Maus, R. Fayt, R. Jérôme and P. Teyssié, *Polymer*, 1995, **36**, 2083.
29 L. Shao, R. A. Weiss and R. D. Lundberg, *J. Polym. Sci., Part B: Polym. Phys.*, 1995, **33**, 2083.
30 D. G. Peiffer, J. Kaladas, I. Duvdevani and J. S. Higgins, *Macromolecules*, 1987, **20**, 1397.
31 I. Capek, *Adv. Colloid Interface Sci.*, 2005, **118**, 73.
32 G. Broze, R. Jérôme, P. Teyssié and C. Marco, *Macromolecules*, 1983, **16**, 996.
33 R. D. Lundberg and R. R. Phillips, *J. Polym. Sci., Part B: Polym. Phys.*, 1982, **20**, 1143.
34 G. Broze, R. Jérôme and P. Teyssié, *Macromolecules*, 1982, **15**, 920.
35 M. R. Tant, G. L. Wilkes and J. P. Kennedy, *J. Appl. Polym. Sci.*, 1989, **37**, 2873.
36 C. Chassenieux, J. F. Tassin, J. F. Gohy and R. Jérôme, *Macromolecules*, 2000, **33**, 1796.
37 C. Chassenieux, T. Nicolai, J. F. Tassin, D. Durand, J. F. Gohy and R. Jérôme, *Macromol. Rapid Commun.*, 2001, **22**, 1216.
38 I. A. Nyrkova, A. R. Khokhlov and M. Doi, *Macromolecules*, 1993, **26**, 3601.
39 L. Leibler, M. Rubinstein and R. H. Colby, *J. Phys. II*, 1993, **3**, 1581.
40 X. Wang, M. Goswami, R. Kumar, B. G. Sumpter and J. Mays, *Soft Matter*, 2012, **8**, 3036.
41 J. P. Spatz, S. Sheiko and M. Möller, *Macromolecules*, 1996, **29**, 3220.
42 K. Khougaz, D. Nguyen, C. E. Williams and A. Eisenberg, *Can. J. Chem.*, 1995, **73**, 2086.
43 A. Desjardins, T. G. M. van de Ven and A. Eisenberg, *Macromolecules*, 1992, **25**, 2412.
44 D. Nguyen, X. F. Zhong, C. E. Williams and A. Eisenberg, *Macromolecules*, 1994, **27**, 5173.
45 C. D. Deporter, T. E. Long and J. E. McGrath, *Polym. Int.*, 1994, **33**, 205.
46 (*a*) Z. Fang and J. P. Kennedy, *J. Polym. Sci., Part A: Polym. Chem.*, 2002, **40**, 3662; (*b*) Z. Fang, S. Wang, S. Quing and J. P. Kennedy, *J. Appl. Polym. Sci.*, 2003, **88**, 1516.
47 H.-Q. Xie, D.-G. Liu and D. Xie, *J. Appl. Polym. Sci.*, 2005, **96**, 1398.

48 K. Xu, K. Li, P. Khanchaitit and Q. Wang, *Chem. Mater.*, 2007, **19**, 5937.
49 X. Lu, W. P. Steekle Jr. and R. A. Weiss, *Macromolecules*, 1993, **26**, 6525.
50 C. Wu, K. Woo and M. Jiang, *Macromolecules*, 1996, **29**, 5361.
51 M. Moffitt, K. Khougaz and A. Eisenberg, *Acc.Chem. Res.*, 1996, **29**, 95.
52 J.-F. Berret, Y. Séréro, B. Winkelman, D. Calvet, A. Collet and M. Viguier, *J. Rheol.*, 2001, **45**, 477.
53 T. Nicolai, O. Colombani and C. Chassenieux, *Soft Matter*, 2010, **6**, 3111.
54 Y. Sèrèro, V. Jacobsen, J.-F. Berret and R. May, *Macromolecules*, 2000, **33**, 1841.
55 M. S. Green and A. V. Tobolsky, *J. Chem. Phys.*, 1946, **14**, 80.